Systems & Control Transactions

Original Research Article
Peer Reviewed Conference Proceeding
ESCAPE 36 - European Symposium on Computer Aided Process Engineering
Sheffield, UK. 21-24 June 2026

PSE PRESS

Optimization-based Design, Simulation and Data-Driven Learning for Resilient Manufacturing Systems

Miriam Sarkis[a*] and Efstratios Pistikopoulos[ab]

[a] Texas A&M University, Energy Institute, College Station, 77843, Texas, United States
[b] Texas A&M University, Artie McFerrin Department of Chemical Engineering, College Station, 77843, Texas, United States
* Corresponding Author: msarkis@tamu.edu

ABSTRACT

Resilience is becoming a top priority across industrial sectors, with increasing pressures to assess it systematically. In this work, we present an optimization-based framework for proactive design and planning under uncertainty of multi-product manufacturing networks, and testing of the reactive strategies available to withstand unforeseen disruptions. Specifically, the design problem is formulated as a two-stage stochastic optimization, integrating multi-period planning and scheduling, aimed towards mitigation against uncertainty. Designs are then fixed and tested through simulated outcomes from *out-of-sample* uncertainty distributions, with feasibility of operation monitored through the time-to-recover post disruption. Infeasibility triggers a scenario-update procedure via K-means clustering, whereby critical uncertainty information based on simulated outcomes is integrated in the proactive planning step, including low-probability high-impact scenarios. Modular and non-modular designs are compared to quantify the value of recourse actions with respect to responsiveness to disruptions. Results highlight that adaptable modular designs enable shorter recovery times combined with lower cost commitments. Overall, the framework underpins the development of tools for the anticipation and mitigation of disruptive events and systematic re-design based on continuously updated uncertainty information.

Keywords: Multiscale Modelling, Planning & Scheduling, Design Under Uncertainty, Stochastic Optimization, Supply Chain, Resilience

INTRODUCTION

As disruptions become the new normal in manufacturing networks operation and management, there emerges a need to develop tools to test and quantify system resilience. In this context, process systems engineering opens opportunities to systematically design process systems under known uncertainty, operate them and test the capacity to withstand emerging unknown disruptive events. Following a disruptive event, data-driven methods offer the opportunity to learn and adapt process system design, integrating feedback from acquired knowledge regarding uncertainty[1].

Proactive strategies to improve resilience involve posing the design problem with respect to expected outcomes of uncertainty. For instance, a stochastic optimization problem is solved based on an approximation of fitted historical data of known demands which correspond to current available uncertainty information. This approach is well established across applications, including chemical supply chains, energy systems and pharmaceuticals [2, 3, 4].

During operation, design decisions are fixed and degrees of freedoms to withstand unforeseen scenarios and disruptive events depend on recourse actions available and the timescale of deployment of such measures. In this reactive planning step, available actions may range from adaptation of schedules to set up of additional capacity. To this end, processes with embedded modularity may allow flexibility to use repurpose and reconfigure equipment trains. Furthermore, modules can also correspond to parallel equipment lines which can be set up to rapidly scale-out/up capacity.

From a modelling perspective, simulation approaches such as rolling horizon [5] in this space are aimed at quantifying the reactive capabilities of a network/process design. In other words, reactive planning can be framed as a simulation of design performance as an *out-*

of-sample test of the first-stage decisions obtained based on the sampled uncertainty in the proactive planning step. Through simulation, significant deviations in target metrics can be monitored, such as service levels and time to recover. Acquired knowledge on system response can be then systematically incorporated in the overall design decisions through a learning step, iteratively re-solving the proactive problem and adjusting design-level decisions. To this end, there emerge opportunities to develop holistic methodological frameworks for the integration of feedback emerging from the reactive-planning part in the proactive layer to obtain better resilience-aware plans/design. This helps quantify resilience as the capacity to both *anticipate* and *respond* to uncertainty.

This study aims to provide a methodological iterative framework for doing so, illustrated on a pharmaceutical manufacturing network case, although transferable to any other batch manufacturing application, undergoing disruptions causing parameter fluctuations. In this work, modular versus non-modular manufacturing equipment cases are systematically compared to quantify the value of recourse capacity installation with respect to cost and adaptability to unforeseen uncertainty.

METHODS

Problem Statement

A capacity planning problem is considered, aimed at minimizing total network-level and scheduling costs. The objective is to evaluate candidate design alternatives based on the ability to anticipate uncertainty and respond under minimal cost and time delay. In this work, a pharmaceutical case study is considered, based on the multi-product manufacturing network shown in Figure 1a and manufacturing-level equipment network shown in Figure 1b. The problem considers:

- A set T of time periods t (daily);
- A subset TT of time periods ts (bi-monthly);
- A set S of states s,
- A subset S^p of product states s,
- A set I of tasks i,
- A set J of equipment j,
- A set A of scales a,
- A set U of parallel modules u,
- A set Ω of demand scenarios d.
- A set M of manufacturing facilities m
- A set K of storage nodes k
- A set L of demand zones l

In this work, multipurpose manufacturing is modelled. Additionally, parallel units can be installed for each equipment. Two alternatives are modelled, namely *modular* manufacturing, under the assumption that equipment can be installed with a time delay, and a *non-modular* option where equipment is installed once and cannot be scaled out in response to variability and disruptions. This effectively corresponds to comparing design with capacity-level recourse actions to fixed designs. The aim of the optimization is to determine the following decisions:

1. Investment in equipment in facilities (F_{jm}),
2. Scale and parallel units ($K_{jamu,ts,d}$, $Y_{jamu,ts,d}$)
3. Task allocation to equipment ($W_{ijamutd}$)
4. State inventories in manufacturing (S_{std})
5. Transport flows ($Q_{sjk,ts,d}$, $Q_{skl,ts,d}$)
6. Sales to meet demands ($Sales_{s,ts,d}$).

Decision 1 is scenario-independent and made at a *first stage*, prior to uncertainty realization. In the modular case, Decisions 2-6 are scenario-dependent and related to operations of the manufacturing network. Hence, these can be defined as *second-stage* decisions, adaptive to scenario realizations. In the non-modular case, Decision 2 is instead a first stage scenario-independent decision.

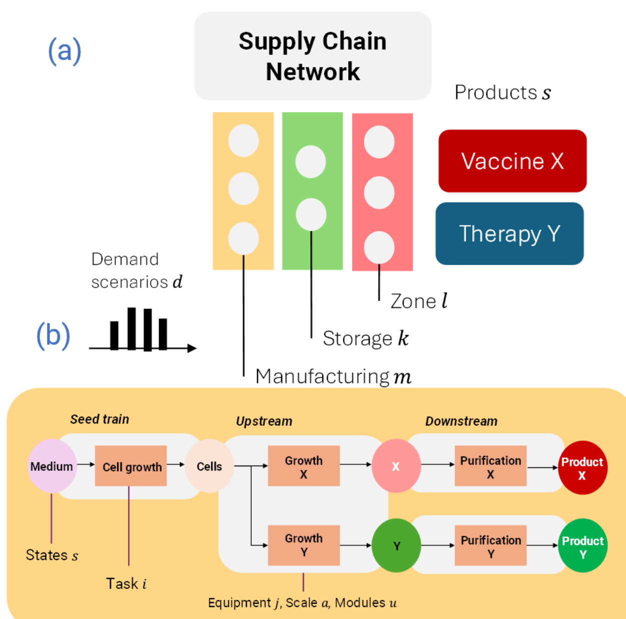

Figure 1. Optimization superstructure at (a) network level, (b) manufacturing process level, integrated supply chain network design and states-task network scheduling.

Algorithm 1: Framework Pseudo Code

Inputs:

- Initial scenario set Ω with probabilities ϕ
- Stress test sample size N_{stress}
- Time-to-recover threshold τ_{TTR}
- Initialize violation set $\Omega^{obs} \leftarrow \varnothing$

Initialize: $\epsilon \leftarrow 0$

while $\epsilon < 10$ do

Solve stochastic optimization problem $(\Omega^{\epsilon}, \phi^{\epsilon})$

Obtain first-stage variables α^{ϵ}, second-stage variables β^{ϵ}

Fix first-stage variables α^{ϵ}

Generate out-of-sample scenarios Ω^{stress}, $|\Omega^{stress}| = N_{stress}$

for each sample $d = 1$ to N_{stress} **do**

Solve deterministic optimization problem

Evaluate time to recover TTR_{pd} for all products p

0 Compute $\widehat{TTR_d} = \max_p TTR_{pd}$

1 **if** $\widehat{TTR_d} \geq \tau_{TTR}$ **then**

2 Let $\Omega^{obs} \leftarrow \{D_1, \ldots, D_n\}$ for both products and $N = d$

3 Partition samples by regime into subsets $\Omega^{obs,r}$

4 Count regime occurrences $N_r = card(\Omega^{obs,r})$

5 Compute empirical regime probabilities $\pi_r = \frac{N_r}{N}$

6 Solve K-means $K_r \coloneqq \min(K, N_r)$ for each regime r

7 Assign scenario realizations: $D_d^X \coloneqq \mu_\kappa^{X,r}, D_d^Y \coloneqq \mu_\kappa^{Y,r}$ for each (k, r)

8 Compute scenario probabilities $\phi_d \coloneqq \pi_r p_\kappa^r$

9 Update scenario tree $(\Omega^{\epsilon+1}, \phi^{\epsilon+1}) \leftarrow \{(D_d^X, D_d^Y, \phi_d)\}_{d=1}^{\Delta}$ with $\Delta = \sum_r K_r$

0 break

1 end if

2 end for

3 $\epsilon \leftarrow \epsilon + 1$

4 end while

Outputs: First-stage design vector α^*

Framework implementation

The workflow for the proactive, reactive planning and scenario updating problem is presented in Algorithm 1. First, a scenario-tree is postulated based on available uncertainty information and a stochastic optimization is solved (Step 3-6).

Iteratively, the obtained design is simulated for samples that are obtained from an unseen distribution, with the aim of testing design feasibility (Step 8-10). If $\widehat{TTR_d}$ is larger than a set threshold τ_{TTR}, the violation is deemed critical, hence the scenario tree is updated (Step 12-19), and the stochastic proactive problem resolved to obtain a new design. Ultimately, the iterative procedure terminates when a first-stage decision vector α^* is optimal with respect to the postulated scenario tree Ω^{ϵ} and feasible with respect to all disruptive scenarios Ω^{Stress}.

Process and demand data

Techno-economic models of manufacturing technologies of interest are developed using the flow sheeting software SuperPro Designer (Intelligen)[5]. Nominal capital, labor and variable cost and process tasks lengths (p_i) are presented in the SI document, for process volumetric scales $a = \{1000, 2000\}$. With respect to demand data, the optimization considers:

$$D_d^Y \sim \mathcal{U}(1000, 2000)\ \forall d = d1, \ldots, d5 \quad (1)$$

$$D_d^X \sim \mathcal{U}(10^6, 2 \times 10^6)\ \forall d = d1, \ldots, d5 \quad (2)$$

Whereby the demand samples are generated by sampling a uniform distribution which represents the knowledge based on historical data of demand patterns. Hence, D_d^X and D_d^Y correspond to samples for demand of product X and Y respectively. These correspond to the initialized scenario tree, with probabilities $\phi_d = \frac{1}{card(D)}$.

Manufacturing level formulation

The scheduling level is formulated as states-task network[6], modifying some constraints to account for scale-dependent (a) and parallel units (u).

Resource balance constraints model the relation between consumption and production ($B_{ijmautd}$) and storage (S_{smtd}) of each resource as follows, for every state s, time period t, facility m, equipment j, scale a and scenario d:

$$S_{smtd} = S_{s,t}^0 + S_{sm,t-1,d} + \sum_i \bar{\rho}_{is} \sum_{j,u,a} B_{ijmau,t-p_{is}d} - \sum_i \rho_{is} \sum_{j,u,a} B_{ijmautd} \quad \forall s, m, t, d \quad (3)$$

Here, it is worth noting that all $\bar{\rho}_{is}$ and ρ_{is} are equal to 1, due to each task modelled as a single state input/output entity (Figure 1b) (SI document).

The amount of material states processed in equipment j, scale a and unit u through task i and time t in scenario d ($B_{ijmautd}$) is bounded by processing constraints, which also are tied to task allocation, via the binary of task-equipment allocation ($W_{ijmautd}$).

$$V_{ija}^{min} W_{ijmautd} \le B_{ijmautd} \le W_{ijmautd} V_{ija}^{max} \; \forall i,j,m,a,u,t,d \quad (2)$$

It is worth noting that each of these operational variables is scenario dependent d and made network-node dependent m, scale dependent a and unit u dependent through the respective indices.

Furthermore, task allocation is constrained by the following equation, which models the logic of equipment occupancy for equipment j at scale a and in unit u once a task is allocated, for the length of its duration p_i.

$$\sum_i \sum_{t'=t}^{t-p_i+1} W_{ijmaut'd} \le 1 \; \forall i,j,m,a,u,t,d \quad (4)$$

Resource storage constraints model the bound on inventory for each state, with a capacity limit (C_s):

$$0 \le S_{smtd} \le C_s \; \forall s,m,t,d \quad (5)$$

Task allocation occurs only within installed equipment, which is modelled through the following constraint:

$$W_{ijmautd} \le Y_{jmau,t_s(t),d} \; \forall i,j,m,a,u,t,d \quad (6)$$

Where $t_s(t) = \max\{t' \in T^m : t' \le t\}$, hence corresponds to the month period ts that encompasses day t.

Equipment installation occurs only within installed facilities suited to produce equipment j at scale a (F_{jma}):

$$Y_{jmau,ts,d} \le F_{jm} \; \forall i,j,m,a,u,ts \in TT,d \quad (7)$$

In the modular case modules can be additionally installed through investment decisions and available after a lead time of 60 days :

$$Y_{jmau,ts,d} = Y_{jmau,ts,d} + K_{jmau,ts-60,sd} \; \forall i,j,m,a,u,ts \in TT,d \quad (8)$$

In the non-modular case, no new investment is possible and availability is carried forward:

$$Y_{jmau,ts,d} = Y_{jmau,ts,d} \; \forall i,j,m,a,u,ts \in TT,d \quad (9)$$

Additionally, line installation is not scenario dependent, but rather an investment made as a first-stage decision, hence fixed across scenarios via the following set of additional constraints:

$$Y_{jmau,ts,d1} = Y_{jmau,ts,d'|d' \neq d1} \; \forall i,j,m,a,u,ts,d' \quad (10)$$

Network level formulation

At supply chain level, inventory balance constraints model the shipment from manufacturing facilities to storage facilities. For the states that are only produced (s^P):

$$S_{smtd} = S_{s,t}^0 + S_{sm,t-1,d} + \sum_i \bar{\rho}_{is} \sum_{j,u,a} B_{ijmau,t-p_{is}d} - \sum_k Q_{smk,ts,d} \; \forall s^P,m,t,d \quad (11)$$

Where, the outbound flow of manufacturing is considered as a consumption term ($Q_{smk,ts,d}$). Shipments to storage facilities k feed into the following equation which models the storage at each facility:

$$\sum_m Q_{smk,ts,d} = \sum_l Q_{skl,ts,d} \; \forall s \in S^P,k,ts \in TT,d \quad (12)$$

In this work, product inventory is not considered and these flow variables are matched only at time periods within the set TT, thus forcing shipments to only occur at time periods ts.

Transport flows from each storage facility feed into demand zones, where demand is fulfilled. Hence:

$$\sum_k Q_{skl,ts,d} = S_{sl,ts,d} \; \forall s \in S^P,l,ts \in TT,d \quad (13)$$

The following sales-demand constraint ensures the amount of doses sold for both product states, at each demand zone l and time period t within the mid term horizon is greater than the demand in each scenario:

$$Sales_{sl,ts,d}\delta_s \ge D_{sl,ts,td} \; \forall s \in S^P,l,ts \in TT,d \quad (14)$$

The demand in each demand zone is calculated based on the total demand sampled, previously computed:

$$D_{sl,ts,d} = \frac{D_d^s}{card(l)} \forall s \in S^P,l,ts \in TT,d \quad (15)$$

Objective function

The total cost of the supply chain is calculated as a function of the capital, labor, variable manufacturing costs and logistics costs:

$$\begin{aligned} \min Expected\,COST \; = & \sum_{jm} c_j^{FAC} F_{jm} \\ & +[\sum_{ijtaumd} \phi_d c_{jai}^{MOD}(Y_{jmautd}) + \sum_{ijtaumd} \phi_d c_{jai}^{LAB}(W_{ijtaumd}) \\ & \sum_{ijtaumd} \phi_d c_{jai}^{VAR}(B_{ijtaumd}) + \sum_{std} \phi_d c_s^{STOR}(S_{std})] \\ & + \sum_{sltd} \phi_d c^P(\eta_{sltd}) + \sum_{smktd} c^T \lambda_{mk} Q_{smktd} + \sum_{skltd} c^T \lambda_{kl} Q_{skltd} \end{aligned} \quad (16)$$

Where the expected cost is sum of scenario-independent investment and scenario-dependent weighted average sum over the operational, transport, storage decisions and, in the modular case, capacity expansion. Here, $c_{ja}^{FAC}, c_{jai}^{MOD}, c_{jai}^{LAB}, c_{jai}^{VAR}, c_s^{STOR}, c^P, c^T$ correspond to the capital, facilities dependent, labor, variable, storage and penalty cost coefficients respectively.

Optimization-based Simulation

The first-stage decisions are fixed and the violation of the sales demand constraint is monitored and penalized. Hence Equation 14 is modified as follows:

$$Sales_{sl,ts,d}\delta_s + \eta_{sl,ts,d} \ge D_{sl,ts,d} \; \forall s,l,ts \in TT,d = d1 \in \Omega^{Stress} \quad (17)$$

The time to recover TTR is the minimum time required to restore service after a disruption, corresponding to the last time period and the first time period undergoing disruption:

$$TTR_{sd} = \max\{ts \in TT, | \sum_l \eta_{sl,ts,d} > 0\} - \min\{ts \in TT, | \sum_l \eta_{sl,ts,d} > 0\} \; \forall s, d = d1 \in \Omega^{Stress} \quad (18)$$

In the simulation step, the objective function (Equation 16) is modified with the addition of a penalty term calculated as function of the shortage of therapies.

$$\min Expected\, COST = \sum_{jm} c_j^{FAC} F_{jm} + [\sum_{ij,ts,aumd} \phi_d c_{jai}^{MOD}(Y_{jmau,ts,d}) + \sum_{ijtaumd} \phi_d c_{jai}^{LAB}(W_{ijtaumd}) + \sum_{ijtaumd} \phi_d c_{jai}^{VAR}(B_{ijtaumd}) + \sum_{std} \phi_d c_s^{STOR}(S_{std})] + \sum_{sl,ts,d} \phi_d c^P(\eta_{sl,ts,d}) + \sum_{smk,ts,d} c^T \lambda_{mk}(Q_{smk,ts,d}) + \sum_{skl,ts,d} c^T \lambda_{kl}(Q_{skl,ts,d}) \quad (19)$$

Upon simulation of reactive planning, the scenario set is reduced to $\{d1\}$, with demand levels assigned iteratively to out-of-samples generated in Ω^{stress}. Hence, demands are generated from out-of-sample distributions:

$$D_d^Y \sim \mathcal{U}(1000, 3000) \; \forall d = d1 \quad (20)$$

Whereby the bounds of the monthly demands for Product Y are modified (Figure 2a).

Additionally, the disruptive regime for Product X is generated based on conditional probability theory, considering a bimodal distribution of demands, where the modes are defined by the sample regime R_d (Figure 2b):

$$R_d \sim Bernoulli(p_{Disruption}),\; p_{Disruption} = 0.04 \; \forall d = d1 \quad (21)$$

$$D_d^X = \begin{cases} Z_d^{disruption}, if\ R_d = 1 \\ Z_d^{Normal}, if\ R_d = 0 \end{cases} \quad (22)$$

Where:

$$Z_d^{disruption} \sim \mathcal{N}(\mu_{disruption}, \sigma_{disruption}^2),$$

$$\mu_{disruption} = 8 \times 10^7, \sigma_{disruption}^2 = 2 \times 10^7 \quad (23)$$

$$Z_d^{Normal} \sim \mathcal{N}(\mu_{Normal}, \sigma_{Normal}^2)$$

$$\mu_{Normal} = 7 \times 10^6, \sigma_{disruption}^2 = 1 \times 10^6 \quad (24)$$

Scenario tree update

The scenario tree update mimics the concept of learning from the demand observed throughout the time horizon. K-means clustering allows systematic grouping collected data in set of K clusters, selected equal to the number of scenarios to build the tree for stochastic optimization and cluster heights used to scale scenario probabilities, whilst also accounting for regime information that enable partition of the samples and construction of regime-specific clusters. Here, $\Omega^{Obs} = \{(D_d^X, D_d^Y, r_d)\}_{d=1}^N$ is the set of demand samples d observed up to iteration ϵ with a recorded corresponding regime. The samples belonging to each regime can be defined as the subsets:

$$\Omega^{Obs,r} = \{(D_d^{X,r}, D_d^{Y,r}) : r_d = r\} \quad (25)$$

The number of occurrences of regime r is defined as:

$$N_r = \mathrm{card}(\Omega^{Obs,r}) \quad (26)$$

Hence, the empirical probability of regime r is the ratio of samples when the regime N_r realizes and the total N:

$$\pi_r = \frac{N_r}{N} \quad (23)$$

For each regime, K-means clustering is performed by solving:

$$\min_{\mu_\kappa^r} \sum_{\kappa=1}^{K_r} \sum_{d \in C_\kappa^r} \left\| \begin{pmatrix} D_d^X \\ D_d^Y \end{pmatrix} - \mu_\kappa^r \right\|^2 \quad (27)$$

Where the C_κ^r is the set of samples d assigned to cluster κ under regime r and μ_κ^r is the centroid of cluster κ under regime r, corresponding to the vector $\begin{pmatrix} \mu_\kappa^{X,r} \\ \mu_\kappa^{Y,r} \end{pmatrix}$ with respect to each product X and Y. The number of clusters per regime is therefore defined as:

$$K_r := \min(K, N_r) \quad (28)$$

Through Equation 28, if a new regime is discovered, N_r new leaves of the scenario tree are added if N_r is below that of the target number K of clusters, which in this work equals 3. Otherwise, K-means yields K scenarios for the each detected regime. The resulting scenario tree probabilities would be adjusted by regime-specific probabilities which are also computed based on collected data during the reactive stage. Therefore, once solved, K-means yields the new scenario realizations, which are reassigned as equal to the identified cluster centroids μ_r^k. Each cluster (k, r) defines a scenario d.

$$D_d^X := \mu_\kappa^{X,r} = \frac{1}{|C_\kappa^r|} \sum_{d \in C_\kappa^r} D_d^{X,r}$$

$$D_d^Y := \mu_\kappa^{Y,r} = \frac{1}{|C_\kappa^r|} \sum_{d \in C_\kappa^r} D_d^{Y,r} \quad (29)$$

New scenario probabilities can be derived from the empirical regime probabilities and the probabilities p_k^r of cluster k for each regime r are calculated as the number of samples that fall under cluster C_k^r and the occurrence of regime r:

$$p_\kappa^r = \frac{card(C_\kappa^r)}{N_r} \quad (30)$$

Hence, overall scenario probabilities are obtained as:

$$\phi_d := \phi_\kappa^r = \pi_r p_\kappa^r \quad (31)$$

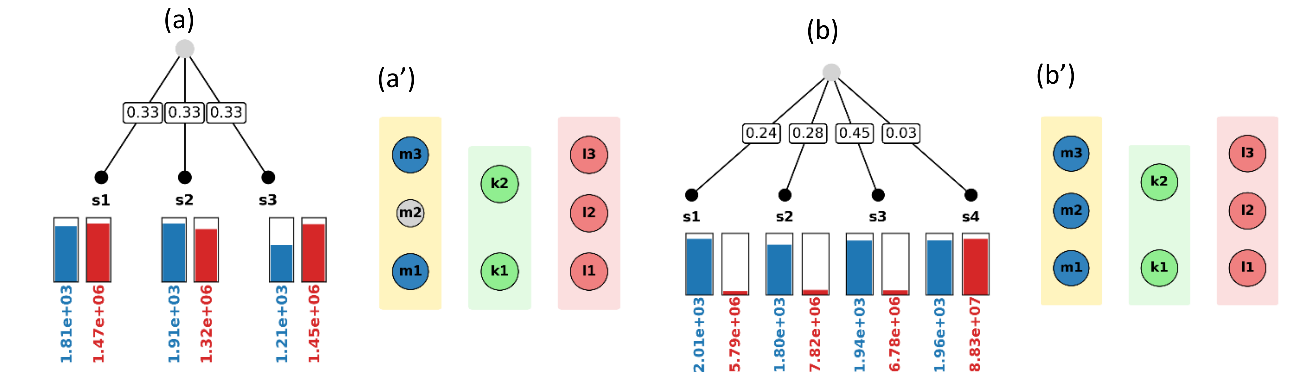

Figure 2. Inputs and first-stage outputs of iterative workflow (a) scenario tree for Iteration 1 (initialization, $\Omega = \Omega^1, \phi = \phi^1$), (a') network-level optimized design for iteration 1, (b) updated scenario tree for iteration 2 (K-means generated, $\Omega = \Omega^2, \phi = \phi^2$), (b') network-level optimized design for iteration 2.

COMPUTATIONAL STATISTICS

The framework is built in Python 3.11 implementing the PYOMO package. The MILP is solved with GUROBI v11 on a Intel(R) Core(TM) i7-10700 CPU @2.90 GHz machine with 64.0 GB RAM. Table 1 presents the computational time for the modular and the non-modular case. It is worth noting that both result in the same number of variables and different computational times across iterations, as the non-modular case is solely obtained by fixing binaries of equipment activation across scenarios (Equation 10), rather than reformulating the problem.

Table 1: Computational Statistics

Iteration	Metric	Modular	Non-modular
1	*CPUs*	236.1	170.11
	Continuous	522	522
	Integer	62,061	62,061
	Constraints	62,595	62,595
2	*CPUs*	690.78	443.14
	Continuous	696	696
	Integer	82,701	82,701
	Constraints	83,409	83,409

Statistics are reported for the proactive solution stage, The reactive stage was found to lead to computational times of $< 1s$, with CPUs reduced due to the fixing of the design degrees of freedom, speeding up convergence.

RESULTS & DISCUSSION

The proposed framework provides a platform to test design feasibility and adaptation capacity to unforeseen uncertainty. Figure 2a presents the initializing scenario tree, which corresponds to equiprobable scenarios sampled from the distributions presented in Equation 1-2. This results in first-stage network-level decisions which are equivalent in the modular and non-modular case (Figure 2a'), corresponding to two facilities installed, namely $m1$ and $m3$, minimizing transport cost and distance travelled, and fulfilling the expected demands. It is worth noting that first-stage equipment-level decisions for the modular and non-modular decisions differ and this is displayed in Figure 3a and Figure 3b, at time period $t = 0$, with different equipment lines installed in terms of scale and parallel units. This is due to the fact the modular equipment allows for ad-hoc installation of capacity as second-stage decisions, whilst the non-modular case considers that the installed equipment is fixed and should fulfill the postulated demand scenarios.

Fixing these case-specific first-stage decisions, stress testing allows the quantification of the adaptive capability of each alternative. In Figure 4a-a' the outcomes of stress testing are highlighted with respect to each product. For each demand realization highlighted in black, modular and non-modular options yield a feasible solution, whereby feasible corresponds to a network that ensures supply given the installed equipment capacity (non-modular case) or through installation of additional units. This is done minimizing cost and time to recover, and, if feasible, the time to recover is below the threshold of $\tau_{TTR} = 120\ days$. Instead, samples highlighted in red are those that trigger this infeasibility, corresponding to a 1900 doses of Y and critically, a 10-fold increase in demand for X, which in this case study corresponds to low-probability, high impact occurrence of a pandemic.

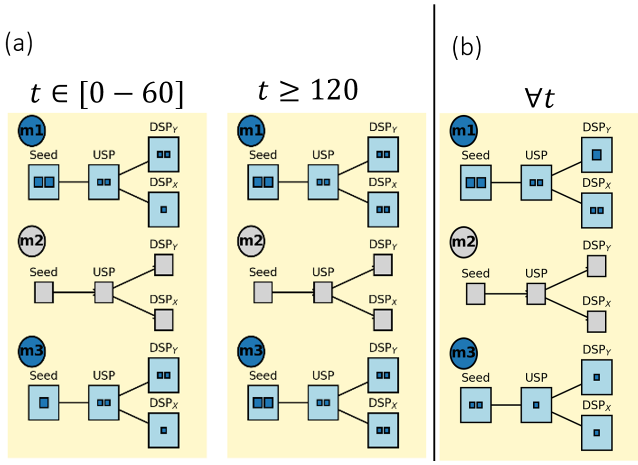

Figure 3. Equipment-level decisions: (a) modular case, (b) nonmodular case fixed equipment structures. Line activated (■), facility inactive (■). Number of lines u and scale a is illustrated for each process equipment type j.

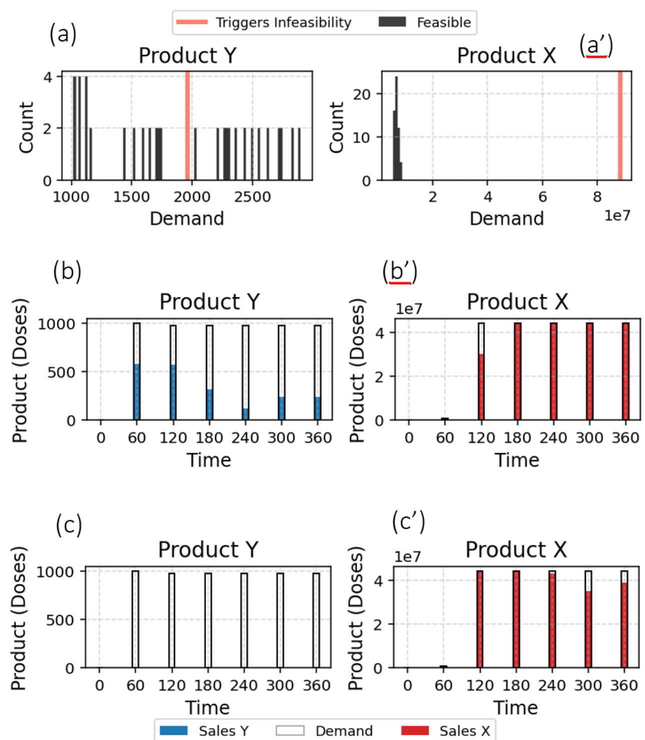

Figure 4. Infeasibility detection: (a) demand for Y, (a') demand for X, (b-b') time to recover in modular case, (c-c') time to recover in non-modular case.

As can be seen in Figure 4b-b', in the modular case, the disruption occurrence causes a $\widehat{TTR_d}$ with respect to product X of approximately $300\,days$ and a minimized $\widehat{TTR_d}$ of $60\,days$ with respect to X. Shortages are even more significant in the non-modular case, with delays of shortages of 120 days on the X side (Figure 4c') and unfulfilled demands on the Y side (Figure 4c).

The response capabilities of the network are seen in Figure 3a and b, where the adaptation of the second-stage decisions is displayed for $t > 60\,days$. In the modular case (Figure 3a), a scale-out of seed capacity and additional DSPx lines to cater for the increased X demand. This leads to the service levels seen in Figure 3b' for X, which are attainable without compromising on capacity for the manufacturing of Y. This then leads to a $\widehat{TTR_d}$ which still does not satisfy the feasibility check; however, it is less significant than in the fixed non-modular case. Figure 3b illustrates instead a fixed structure that is not scenario dependent on the entirety of the time horizon, hence the only degrees of freedoms to respond to disruptions become the adjustments of the operational planning decisions. This leads to more significant shortages and longer $\widehat{TTR_d}$ times in the non-modular case.

Additionally, Figure 2b highlights how post-infeasibility, K-means clustering generates a new scenario tree, systematically incorporating 1 new leaf, which corresponds to the detected 1 low-probability (0.03) high impact $(8.37e8\,doses)$ scenario representing the *disruption* regime, and adjusted probabilities based on the realized demands for the *normal condition* regime. Solving the stochastic optimization again leads to adjusted first-stage decisions, which also embed the activation of facility $m2$ (Figure 2b')

Based on the updated design, the simulated stress test is repeated, resulting in feasibility for all samples within Ω^{Stress}, for both the modular and non-modular case. Then, it becomes worth comparing the costs of optimality and feasibility. In Figure 5a, the costs for the modular case is displayed, with iteration 1 resulting in costs of $8.3M\ USD/y$ for facility capital-investment related decisions. The CapEx of the module investment $(90M\ USD/y)$, the variable $(11M\ USD/y)$ and labor costs $(6M\ USD/y)$ are second-stage because dependent on operation and scenario realization and therefore not-committed a priori. Instead, in the non-modular case, the equipment is installed and fixed, hence the total displayed CapEx of $12.8M\ USD/y + 131.9M\ USD/y$ is a cost-commitment taken prior to scenario realization and larger, as expected to cater for all demand occurrences, including increased demands with additional capacity.

Stress testing in Iteration 1, highlights that in both the modular and non-modular case the expected cost can increase, due to realization of larger demands not captured in the scenario tree. Specifically, the outlier on the modular case corresponds to the sample displayed in Figure 4b-b', where increased production levels to minimize shortages lead to higher costs. At Iteration 2 the expected optimal costs in both cases result higher based on an updated scenarios that capture the observed samples in the previous iteration, until infeasibility was detected. Added cost results from idle equipment in $m2$, catering for disruptions and increased demand resulting from it; expected modular costs remain lower.

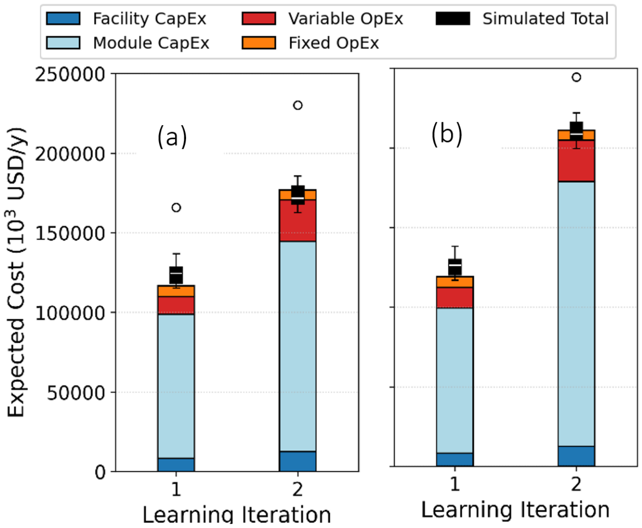

Figure 5. Expected and simulated costs for (a) modular, (b) non modular case over iterations

It emerges that flexibility of rapid scale-out allows minimization of cost commitments and better adaptability to disruption scenarios. Hence, the presented comparison between modular and non-modular equipment is fundamentally a theoretical comparison on benefit of recourse actions in ensuring cost-effective anticipation and response to disruptive events that impact the system.

Based on the results presented, there emerge avenues of development of the optimization-based assessment platform. First, the reactive planning part solves a deterministic optimization problem which assumes perfect foresight of the disruption realizing at time $t = 60$. Hence the TTR is computed optimistically, based on deterministic disruption anticipation and mitigation. Nevertheless, solving this part through a rolling horizon optimization would correspond to a more-realistic response characterization as part of the feasibility test. Second, expected cost was primarily used as performance indicator when comparing the two manufacturing alternatives. Sustainability metrics for capacity establishment and operation could be integrated in the optimization constraints: the former would account for footprint of facility establishment, multiplied by the selection of binary installment variables (e.g. $Y_{jmau,ts,d}$) and the latter accounting for footprint scaling production levels (e.g. $B_{ijtaumd}$) and resource use (e.g. heat and electricity).

Overall, the proposed tool enables process design resilience assessment prior to deployment at scale and during operation. On the one hand, the modelling platform could support comparative assessments, as shown in this study, to identify good design candidates that perform cost-effectively in response disruptions. On the other hand, the tool could be deployed as a back-end simulator, with testing for a continuously updated set of disruptive events and anticipation of re-design priorities prior to disruptions striking in real life scenarios.

CONCLUSIONS

Resilience is becoming a growing priority across industrial sectors, with pressures to design systems that are adaptive to evolving uncertainty from diverse sources. In this work, we develop a framework for proactive design under a priori postulated uncertainty and testing for adaptation to unforeseen uncertainty through simulation. This is achieved through an *out-of-sample* optimization-based simulation from distributions that describe occurrences of disruptive events impacting demand scale for the products. To update uncertainty information when significant service loss due to disruptions emerge, scenario clustering techniques are leveraged to allow updating of the scenario tree, updating uncertainty information worth integrating in the design steps.

The capabilities of the framework are shown comparing examples of modular and non-modular manufacturing equipment designs, highlighting the value of recourse capacity expansion which the former option offers, alongside to initial lower cost commitments. Overall, the tool enables comparative analyses towards the establishment of more resilient designs centered around continuous improvement via systematic uncertainty-related data, making it a valuable tool in real-time simulation of future disruptions through anticipation, mitigation and adaptation of process/network design.

DIGITAL SUPPLEMENTARY MATERIAL

Supplementary information including nomenclature and input data used is available at **LAPSE:2026.0044**.

ACKNOWLEDGEMENTS

Financial support from the Texas A&M Energy Institute is gratefully acknowledged.

REFERENCES

1. Chrisandina NJ, Vedant S, Iakovou E, Pistikopoulos EN, El-Halwagi MM. Metrics and methods for resilience-aware design of process systems: advances and challenges. Current Opinion in Chemical Engineering 43:100984 (2024). https://doi.org/10.1016/j.coche.2023.100984
2. Marques CM, Moniz S, de Sousa JP, Barbosa-Póvoa AP. A simula-tion-optimization approach to integrate process design and planning decisions under technical and market uncertainties. Comput Chem Eng. 106:796-813.(2017) https://doi:10.1016/j.compchemeng.2017.04.008
3. Efthymiadou ME, Charitopoulos VM, Papageorgiou

LG. Optimization approach for hydrogen infrastructure planning under uncertainty. Ind. Eng. Chem. Res. 64:7431-7451 (2025). https://doi.org/10.1021/acs.iecr.4c04211
4. Guillén?Gosálbez G, Grossmann IE. Optimal design and planning of sustainable chemical supply chains under uncertainty. AIChE Journal 55:99-121 (2008). https://doi.org/10.1002/aic.11662
5. Sarkis M, Shah N, Papathanasiou MM. Characterization of key manufacturing uncertainties in next generation therapeutics and vaccines across scales. J Adv Manuf Process. 5: e10158 (2023) https://doi:10.1002/amp2.10158
6. Kondili E, Pantelides CC, Sargent RWH. A general algorithm for short-term scheduling of batch operations—i. MILP formulation. Computers & Chemical Engineering 17:211-227 (1993). https://doi.org/10.1016/0098-1354(93)80015-f